Inorg. Chem. **2007**, *46*, 2243–2248

Multiple Photochemical Reaction Pathways in a Ni(II) Coordination Compound

Franklin P. Ow, Bryana L. Henderson, and Jeffrey I. Zink*

Department of Chemistry and Biochemistry, University of California, Los Angeles, Los Angeles, California 90095

Received October 13, 2006

The gas-phase photofragmentation of the mixed-ligand coordination compound *trans*-bis(trifluoroacetato)bis(*N*,*N*′-dimethylethylenediamine)nickel(II) ($Ni(tfa)_2(dmen)_2$) detected via time-of-flight mass spectrometry is reported. In contrast to most gas-phase studies of metal-containing compounds where fragmentation of weak metal–ligand bonds dominates, the data here show that the dmen ligands fragment while still coordinated to nickel. The manner in which these ligands fragment is highly specific, leading to mono- and diimine species that remain coordinated to nickel. Uncoordinated mono- and diimine species and various small dmen fragments are also observed with high intensities in the low mass region of the spectra. NiF^+, a fragment that is formed by fluorine abstraction, is always observed, even though no Ni–F bonds exist in the starting material.

Introduction

Photochemical reactions of transition metal coordination compounds in solution have been studied extensively and typically involve photosubstitution (commonly photosolvation) and photoredox (usually metal oxidation).[1−14] Studies of the photochemical reactivity of Ni(II) complexes are relatively rare;[15−21] photoelimination of a ligand is a common reaction pathway. In first row transition metal coordination compound photochemistry, photosubstitution and photoelimination almost always involve breaking a metal−ligand bond.[1−4,17−19] Only in rare instances involving reactive ligands is internal ligand bond breaking important (e.g., N−N bond breaking in an azido ligand to form a coordinated nitrene and dinitrogen).[10]

Gas-phase photochemistry of metal-containing compounds has focused primarily on organometallic compounds because uncharged molecules containing small organic ligands often are relatively volatile. The most thoroughly studied gas-phase photochemical reactions to date have been those of metal carbonyl compounds[22−29] and of metallocenes.[30−35] Nickel

* To whom correspondence should be addressed. E-mail: zink@chem.ucla.edu. Tel: 310-825-1001. Fax: 310-206-4038.

(1) Sykora, J.; Sima, J. *Photochemistry of Coordination Compounds*; Elsevier: Amsterdam, 1990.
(2) Geoffroy, G. L; Wrighton, M. S. *Organometallic Photochemistry*; Academic Press: New York, 1979.
(3) Adamson, A. W.; Fleischauer, P. D. *Concepts of Inorganic Photochemistry*; Wiley-Interscience: New York, 1970.
(4) (a) Zink, J. I. *J. Am. Chem. Soc.* **1972**, *94*, 8039−8046. (b) Zink, J. I. *Inorg. Chem.* **1973**, *12*, 1957−1959. (c) Incorvia, M. J.; Zink, J. I. *Inorg. Chem.* **1974**, *13*, 2489−2494.
(5) Bitterwolf, T. E. *Coord. Chem. Rev.* **2006**, *250*, 388−413.
(6) Zink, J. I. *Coord. Chem. Rev.* **2001**, *211*, 69−96.
(7) Vlcek, A. *Coord. Chem. Rev.* **1998**, *177*, 219−256.
(8) Adamson, A. W. *Catal. Met. Complexes* **1993**, *14*, 1−14.
(9) Bergamini, P.; Costa, E.; Sostero, S.; Traverso, O. *Coord. Chem. Rev.* **1993**, *125*, 53−62.
(10) Sima, J. *Coord. Chem. Rev.* **2006**, *250*, 2325−2334.
(11) Vogler, A.; Kunkely, H. *Coord. Chem. Rev.* **2000**, *208*, 321−329.
(12) Kirk, A. D. *Chem. Rev.* **1999**, *99*, 1607−1640.
(13) Balzani, V.; Credi, A.; Venturi, M. *Coord. Chem. Rev.* **1998**, *171*, 3−16.
(14) Kajitani, M.; Fujita, T.; Hisamatsu, N.; Hatano, H.; Akiyama, T.; Sugimori, A. *Coord. Chem. Rev.* **1994**, *132*, 175−180.
(15) Lundmann, M. F.; Wagestian, F.; Dartiguenave, M.; Dartiguenave, Y. *Inorg. Chim. Acta* **1980**, *41*, 253.
(16) Ivin, K. J.; Jamieson, R.; McGarvey, J. J. *J. Am. Chem. Soc.* **1972**, *94*, 1763.
(17) Prakash, H.; Natarajan, P. *Res. Chem. Intermed.* **2003**, *29*, 349−364.
(18) Lewis, F. D.; Miller, A. M.; Salvi, G. D. *Inorg. Chem.* **1995**, *34*, 3173−3181.
(19) Ngai, R.; Wang, Y. H. L.; Reed, J. L. *Inorg. Chem.* **1985**, *24*, 3802−3807.
(20) Wang, F.; Wu, X.; Finnen, D. C.; Neckers, D. C. *Tetrahedron Lett.* **2000**, *41*, 7613−7617.
(21) Lavallee, R. J.; Bentley, J.; Billing, R.; Hennig, H.; Ferraudi, G.; Kutal, C. *Inorg. Chem.* **1997**, *36*, 5552−5558.
(22) Ashfold, M. N. R.; Howe, J. D. *Annu. Rev. Phys. Chem.* **1994**, *45*, 57−82.
(23) Boesl, U.; Neusser, H. J.; Schlag, E. W. *Chem. Phys. Lett.* **1982**, *87*, 1−5.
(24) Johnson, P. M. *Acc. Chem. Res.* **1980**, *13*, 20−26.
(25) Jackson, R. L. *Acc. Chem. Res.* **1992**, *25*, 581−586.
(26) Schlag, E. W.; Neusser, H. J. *Acc. Chem. Res.* **1983**, *16*, 355−360.
(27) Karny, Z.; Naaman, R.; Zare, R. N. *Chem. Phys. Lett.* **1978**, *59*, 33−37.
(28) Dietz, T. G.; Duncan, M. A.; Liverman, M. G.; Smalley, R. E. *J. Chem. Phys.* **1980**, *73*, 4816−4821.

10.1021/ic061969c CCC: $37.00
Published on Web 02/10/2007

tetracarbonyl, substituted nickel carbonyls, and nickelocene photofragmentation have been reported. Photochemical reactions of organometallic compounds and transition metal coordination complexes in the gas phase are of great interest due to their roles as single-source precursors in laser-assisted chemical vapor deposition.[36−45] Multiphoton ionization of these compounds results in the cleavage of relatively weak metal−ligand bonds (e.g., Ni−O, Ni−N vs ligand-centered C−C, C−H bonds) and dominant formation of the bare metal ion. Photoionization of the parent compound[46−52] is usually a minor process, if observed at all, because fragmentation usually precedes ionization. Furthermore, fragmentation of the coordinated ligand to produce lighter metal-containing fragments is rare.[50] Recent studies from our laboratories have demonstrated that in some cases the parent ion is formed in significant yield.[53−55] The molecules can absorb additional photons resulting in photoproducts that contain fragments of the original ligand that remained coordinated to the metal. In the case of a mixed-ligand cobalt cyclooctadiene compound,[54] the organic ligand fragmented to produce coordinated fragments ranging from two to seven carbons with strong peaks from the ethylene, allyl, and benzene organocobalt compounds.

In this paper we report the first gas-phase photochemical study of a classical "Werner" first row transition metal coordination complex, *trans*-bis(trifluoroacetato)bis(*N*,*N*′-dimethylethylenediamine)nickel(II) ($Ni(tfa)_2(dmen)_2$). There are several unexpected results. First, fragmentation of the dmen ligand occurs while coordinated to nickel. Second, dmen fragments to form specific mono- or diimine products. Finally, diatomic NiF^+ is observed at all wavelengths studied even though no Ni−F bonds exist in the starting material.

Experimental Section

Materials. $Ni(tfa)_2(dmen)_2$ was prepared by the reported procedure.[56] All reagents were commercially available from Aldrich and used without further purification.

Spectroscopy. UV−vis spectra were acquired in methanol in a Varian Cary 5000 UV−vis−NIR spectrophotometer using quartz cuvettes. Photoionization mass spectra were measured at 355 nm (20−65 mJ/pulse, $\sim 10^8-10^9$ W/cm^2) and in the range of 410−610 nm ($\sim$20 mJ/pulse, $\sim 10^8$ W/cm^2). The time-of-flight mass spectrometer (TOF MS) was constructed based on a design in the literature.[57] Photoionization occurs in a stainless steel cube (30 cm edges) equipped with quartz windows and evacuated to less than 10^{-6} Torr by a 6 in. diffusion pump fitted with a water-cooled baffle. $Ni(tfa)_2(dmen)_2$ is sublimed at 85−100 °C before it is seeded in He with a backing pressure of about 10^3 Torr and is admitted to the high-vacuum chamber via a pulsed nozzle. The high-speed solenoid valve (General Valve series-9, 0.5 mm orifice) sends a 0.2 ms pulse of the sublimed sample (entrained in He) to intersect the ionization laser beam at 90°. An OPOTEK optical parametric oscillator (410−680 nm, 6 ns pulse width, $\sim$20 mJ/pulse, 10−20 cm^{-1} bandwidth) pumped by the third harmonic of a Quantel Brilliant Nd:YAG laser is used for excitation. An optional KV-389 filter is used to eliminate residual pump (355 nm) from the visible laser beam. Alternatively, the second harmonic (20−75 mJ/pulse, $\sim 10^8-10^9$ W/cm^2) of the Nd:YAG itself may be used for ionization. The fragment ions are accelerated through a 1 m flight tube kept at 10^{-6} Torr using a Varian V300HT 6 in. air-cooled turbomolecular pump. Accelerator voltages are 3000 V, 2100 V, and ground, respectively, in order from farthest to nearest the detector. Ions are detected using a 40 mm diameter triple microchannel plate detector assembly (R.M. Jordan, Inc.). The ion signal is processed using a Tektronix TDS2022 200 MHz dual channel digital oscilloscope interfaced to a PC.

Results

UV−vis Absorption Spectrum. The absorption spectrum of $Ni(tfa)_2(dmen)_2$ was taken in methanol solution, and peaks were observed at 369 nm, $\epsilon = 13$ M^{-1} cm^{-1}; 600 nm, $\epsilon = 6$ M^{-1} cm^{-1}; and 770 nm, $\epsilon = 1$ M^{-1} cm^{-1} and assigned to the $^3T_{1g}(P) \leftarrow {}^3A_{2g}$, $^3T_{1g}(F) \leftarrow {}^3A_{2g}$, and $^1E_g \leftarrow {}^3A_{2g}$ transitions, respectively.[58]

Photofragmention Caused by 355 nm Excitation. The TOF mass spectra of $Ni(tfa)_2(dmen)_2$ were obtained with 355 nm excitation. In general, the nickel cation at 58 *m*/*z* is dominant under all conditions. There are multiple high mass

(29) Smalley, R. E.; Wharton, L.; Levy, D. H. *Acc. Chem. Res.* **1977**, *10*, 139−145.
(30) Ketkov, S. Y.; Selzle, H. L.; Heinrich, L.; Schlag, E. W. *Isr. J. Chem.* **2004**, *44*, 65−69.
(31) Ketkov, S. Y.; Selzle, H. L.; Heinrich, L.; Schlag, E. W. *Mol. Phys.* **2004**, *102*, 1749−1757.
(32) Ketkov, S. Y.; Selzle, H. L.; Heinrich, L.; Schlag, E. W. *J. Chem. Phys.* **2004**, *121*, 149−156.
(33) Ketkov, S. Y.; Selzle, H. L.; Heinrich, L.; Schlag, E. W.; Titova, S. N. *Chem. Phys.* **2003**, *293*, 91−97.
(34) Ketkov, S. Y.; Selzle, H. L.; Heinrich, L.; Schlag, E. W.; Domrachev, G. A. *Chem. Phys. Lett.* **2003**, *373*, 486−491.
(35) Ketkov, S. Y.; Selzle, H. L.; Heinrich, L.; Schlag, E. W.; Domrachev, G. A. *Inorg. Chem. Comm.* **2002**, *5*, 909−912.
(36) Baum, T. H.; Commita, P. B. *Thin Solid Films* **1992**, *218*, 80−94.
(37) Ehrlich, D. J.; Osgood, R. M., Jr.; Deutsch, T. F. *IEEE J. Quantum Electron.* **1980**, *QE16*, 1233−1243.
(38) Osgood, R. M.; Deutsch, T. F. *Science* **1985**, *227*, 709−714.
(39) Morosanu, C. E. *Thin Films by Chemical Vapor Deposition*; Elsevier: New York, 1990.
(40) Eden, J. G. *Photochemical Vapor Deposition*; Wiley: New York, 1992.
(41) Hitchman, M. L.; Jensen, K. F. *Chemical Vapor Deposition*: *Principles and Applications*; Academic Press: San Diego, 1993.
(42) Kodas, T. T.; Hampden-Smith, M. J. *The Chemistry of Metal CVD*; VCH: Weinheim, and New York, 1994.
(43) Braichotte, D.; Garrido, C.; van den Bergh, H. *Appl. Surf. Sci.* **1990**, *46*, 9−18.
(44) Cheon, J.; Zink, J. I. *J. Am. Chem. Soc.* **1997**, *119*, 3838−3839.
(45) Cheon, J.; Talaga, D. S.; Zink, J. I. *Chem. Mater.* **1997**, *9*, 1208−1212.
(46) Muraoka, P.; Byun, D.; Zink, J. I. *J. Am. Chem. Soc.* **2000**, *122*, 1227−1228.
(47) Cheon, J.; Muraoka, P.; Zink, J. I. *Chem. Mater.* **2000**, *12*, 511−516.
(48) Bitner, T. W.; Zink, J. I. *Inorg. Chem.* **2002**, *41*, 967−972.
(49) Muraoka, P.; Byun, D.; Zink, J. I. *Coord. Chem. Rev.* **2000**, *208*, 193−211.
(50) Gedanken, A.; Robin, M. B.;Kuebler, N. A. *J. Phys. Chem.* **1982**, *86*, 4096−4107.
(51) Jaeger, T. D.; Duncan, M. A. *J. Phys. Chem. A* **2004**, *108*, 11296−11301.
(52) Jaeger, T. D.; Duncan, M. A. *Int. J. Mass Spectrom.* **2005**, *241*, 165−171.
(53) Muraoka, P.; Byun, D.; Zink, J. I. *J. Phys. Chem. A* **2001**, *105*, 8665−8671.
(54) Byun, D.; Zink, J. I. *Inorg. Chem.* **2003**, *42*, 4308−4315.
(55) Ow, F. P.; Berry, M. T.; May, P. S.; Zink, J. I. *J. Phys. Chem. A* **2006**, *110*, 7751−7754.
(56) Senocq, F.; Urrutigoity, M.; Caubel, Y.; Gorrichon, J.-P.; Gleizes, A. *Inorg. Chim. Acta* **1999**, *288*, 233−238.
(57) Wiley, W. C.; McLaren, I. H. *Rev. Sci. Instrum.* **1955**, *26*, 1150−1157.
(58) Agambar, C. A.; Anstey, P.; Orrell, K. G. *J. Chem. Soc., Dalton Trans.* **1974**, 864−869.

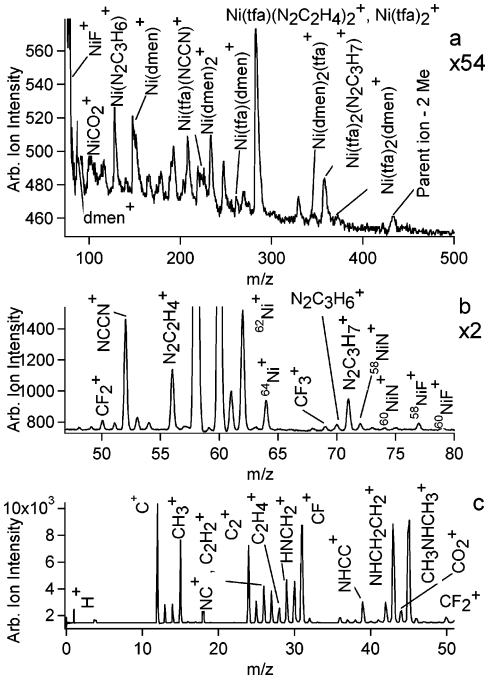

Figure 1. TOF MS of photofragments caused by 355 nm excitation (~10^9 W/cm^2) of *trans*-bis(trifluoroacetato)bis(*N*,*N*′-dimethylethylenediamine)-nickel(II) from (a) 75−500, (b) 47−80, and (c) 0−50 *m*/*z*.

peaks from nickel-containing ions representing dmen fragments that remain coordinated to the metal. Although the parent ion is not observed, the highest mass fragment is the complex with two methyl groups dissociated. Several nickel-containing diatomic fragments are present, along with smaller organic fragments in significant yield. For cases where the exact structure of a fragment is not known, the empirical formula is given. A table listing the observed peaks, their relative intensities, and chemical composition is in the Supporting Information.

Figure 1a shows the TOF MS results between 80 and 500 *m*/*z*. This region consists of metal-containing peaks of the general formula $Ni(tfa)_{0-2}(N_2C_xH_y)_{0-2}^+$ ($x = 2-4$ and $y = 0-12$). The most intense peak in this high mass region is broad and spans the range of 282−286 *m*/*z*, with likely contributions from either $Ni(tfa)_2^+$, $Ni(tfa)(N_2C_2H_4)_2^+$, or both. The latter is probable, since loss of various amounts of hydrogens can easily contribute to peak broadness. These signals are nearly twice as intense as any of the other peaks in this region. As will be discussed later, these heavy mass peaks can be produced by several different photofragmentation pathways from the parent compound. Nickel isotopes are not resolved for heavy nickel-containing species. A longer flight time increases both the probability of collisions and the chance that ions dissociate prior to reaching the detector. In addition, hydrogen loss may result in a cluster of peaks that can mask the nickel isotopes. The results are always broad mass peaks.

Figure 1b is the mass spectrum from 47 to 80 *m*/*z*, and Figure 1c is the mass spectrum from 0 to 50 *m*/*z*, both under the same conditions as Figure 1a. The naturally occurring isotopes of nickel (58, 60, 61, 62, and 64 *m*/*z*) are always observed, and the most abundant isotopes ($^{58}Ni^+$ and $^{60}Ni^+$) are off scale under this magnification. The ^{58}NiF and ^{60}NiF

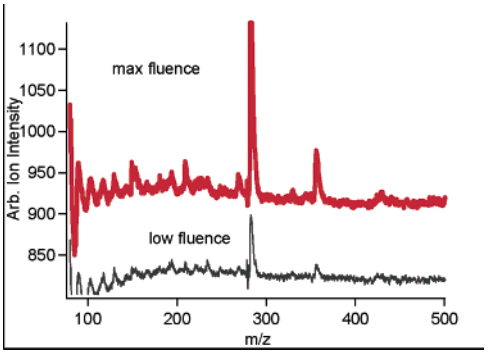

Figure 2. TOF MS at 355 nm under both low (~10^8 W/cm^2) and high (~10^9 W/cm^2) fluence conditions. The most sensitive ions are between 282 and 286 *m*/*z* (3 photon dependence).

isotopes of diatomic NiF^+ (77, 79 *m*/*z*) are resolved. Although minor mass peaks at 72, 74 *m*/*z* and 74, 76 *m*/*z* may be attributed to NiN^+ and NiO^+, respectively, ions which have identical masses complicate the assignments (e.g., $N_2C_3H_8^+$, 72 *m*/*z*). Three notable ligand fragments are seen at 52, 56, and 71 *m*/*z*, referring to dicyanogen ($NCCN^+$), $N_2C_2H_4^+$, and $N_2C_3H_7^+$, respectively. Each originates from the dmen ligand (discussed in further detail below). Mass signals assigned as CF_{1-3}^+ (31, 50, 69 *m*/*z*) are observed, with CF^+ nearly 10 times as intense as CF_2^+ and CF_3^+. The only other mass signal specifically arising from the tfa ligand is CO_2^+ (44 *m*/*z*). In general, the ligand fragment intensities below 50 *m*/*z* ($N_{0,1}C_{1,2}H_{0-7}^+$) from Figure 1c are more intense than the heavier mass peaks (above 50 *m*/*z*). C^+ is always the most dominant ligand fragment.

The effects of varying laser fluence on the overall yields of NiF^+ and Ni^+ were studied at 355 nm excitation. Log−log plots (see Supporting Information) showing the power dependence of these ions were obtained. A 3.3 photon dependence is observed for Ni^+ production, whereas a 1.9 photon dependence is calculated for NiF^+ formation. Due to saturation effects, the actual number of photons involved may be larger.[50] The dramatic effect on the mass spectrum caused by varying the fluence is shown in Figure 2. The biggest difference concerns ion production between 282 and 286 *m*/*z*, assigned as either $Ni(tfa)(N_2C_2H_4)_2^+$ or $Ni(tfa)_2^+$, or both. log−log plots of ion intensity versus laser power were also obtained. A 3.0 photon dependence was calculated for the production of these ions.

Photofragmentation Caused by Visible Excitation. In order to characterize wavelength dependencies for the photofragmentation pathways of the parent compound, TOF mass spectra were obtained in the visible region from 410 to 532 nm. The nickel cation is always the dominant peak. The metal-containing high mass ions that are observed with 355 nm excitation are not seen with visible excitation; no peaks with masses greater than 152 *m*/*z* are observed.

1. Excitation between 410 and 500 nm. TOF mass spectra were taken at 426.3, 438.6, and 460.8 nm (see Supporting Information). All spectra taken in this visible wavelength region display the same mass peaks with only slight changes in relative intensities. The nickel isotopes are not resolved. Peaks at 74 and 77 *m*/*z* are assigned as NiO^+ and NiF^+, respectively. The lower resolution and the presence of ions

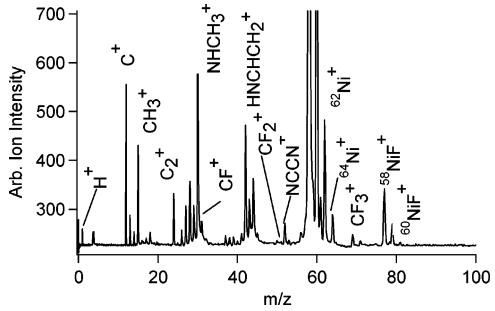

Figure 3. TOF MS at 532 nm ($\sim 10^9$ W/cm^2). Ni^+ is dominant, and the ratio of NiF^+ to smaller inorganic fragments increases.

with similar masses make peak assignment difficult. A broad peak at 88 *m*/*z* is attributed to $dmen^+$ ions with various amounts of hydrogen loss. Spectra taken between 461 and 500 nm display the same peaks but with poorer signal-to-noise ratios.

2. Excitation with 532 nm. The TOF mass spectrum taken at 532 nm between 0 and 110 *m*/*z* is shown in Figure 3. The nickel isotopes are resolved. The only diatomic-nickel-containing species observed is NiF^+. The ratio of NiF^+/Ni^+ increases significantly from that observed at both 355 and 410−500 nm excitations. $^{58}NiF^+$ is now larger than $^{64}Ni^+$, and it is also more abundant than the CF_x^+ ions at 31, 50, and 69 *m*/*z*. The ratio of NiF^+/dmen fragments (52, 56, and 71 *m*/*z*) also increases. The amount of CF_x^+ generated is relatively less at 532 nm than at 355 nm. With UV excitation, CF^+ has a higher ion yield than the dmen fragments between 24 and 30 *m*/*z*. At 532 nm, CF^+ is now hardly observed. The small dmen fragments, $H_{0-5}N_{0-2}C_{0-4}^+$, that are present under 355 nm excitation are also observed at 532 nm. The most dominant organic mass peak is $NHCH_3^+$ at 30 *m*/*z*.

Discussion

Transition metal ions in high oxidation states have the ability to oxidize coordinated amine ligands to mono- and diimine ligands that remain coordinated to the metal, as in the specific case of oxidative ligand dehydrogenation. Examples include organometallic compounds with a variety of mono- and bidentate ligands bound to metals such as iron, copper, nickel, ruthenium, osmium, and platinum.[59−65] These solution-phase studies do not involve photons. Our studies provide an unprecedented case where amine-to-imine transformations occur via multiple photoredox processes in the gas phase. The intensities of the peaks containing coordinated-imine fragments are relatively weak and suggest a minor channel of the general photochemical process. However, the fact that they are observed at all is noteworthy.

Scheme 1. Initial Steps Proposed for the Photofragmentation of $Ni(tfa)_2(dmen)_2$[a]

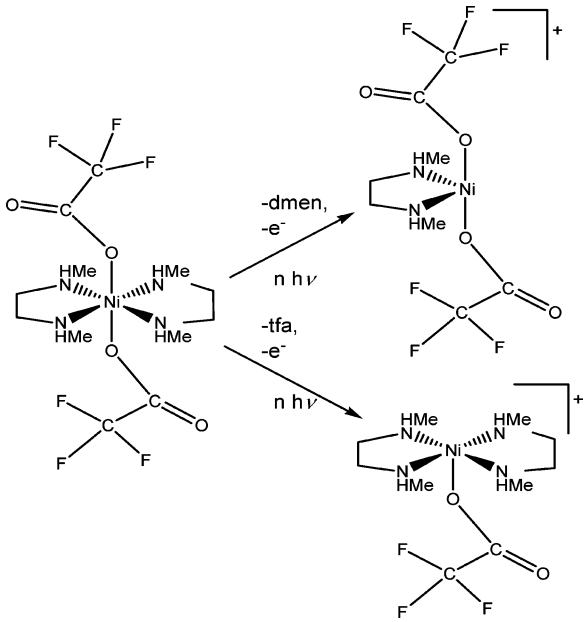

[a] The parent molecule can lose a dmen ligand and retain both tfa groups. The alternate route involves losing a tfa group while both dmen ligands remain attached to Ni.

The gas-phase photofragmentation reactions of $Ni(tfa)_2(dmen)_2$ exhibit surprising features that are unusual in the photodissociation of metal-containing compounds in the gas phase. First, fragmentation of the dmen ligand occurs while it remains coordinated to the metal. In general, for metal-containing compounds, covalent intraligand bonds are stronger than coordinate-covalent metal−ligand bonds[50] (e.g., D(C−O) = 256.7 kcal/mol,[66] D(Ni−O) = 87.4 kcal/mol[67]). Because of this, dmen would be expected to completely dissociate from nickel before any internal rearrangement occurs. Second, dmen not only undergoes fragmentation while remaining bonded to nickel but also fragments in very specific ways. Unexpectedly, many relatively stable mono- or diimine species are observed. Third, NiF^+ is observed under all conditions even though there are no Ni−F bonds in the parent compound.

1. Initial Fragmentation Steps. Two distinct photofragmentation routes are evident (Scheme 1). (It is impossible to determine if observed ions are being formed from neutral parent molecules or from cationic species. One cannot rule out either reaction sequence.) The first pathway is very short and begins with the parent molecule retaining both acid groups and losing one dmen group. The heaviest fragment in this pathway is $Ni(tfa)_2(dmen)^+$ at 372 *m*/*z*. In subsequent steps, both tfa groups can remain coordinated to nickel or one tfa can dissociate. In the former case, mass peaks corresponding to $Ni(tfa)_2(N_2C_3H_7)^+$ (355 *m*/*z*) and $Ni(tfa)_2^+$ (284 *m*/*z*) are observed. In the latter, $Ni(tfa)(dmen)^+$ (259 *m*/*z*) loses the tfa group, resulting in mass peaks of the general formula $Ni(N_2C_{2-4}H_{0-10})^+$.

(59) Bernhard, P.; Bull, D. J.; Burgi, H.-B.; Osvath, P.; Rasilli, A.; Sargeson, A. M. *Inorg. Chem.* **1997**, *36*, 2804−2815.
(60) Sargeson, A. M. *Pure Appl. Chem.* **1986**, *58*, 1511−1522.
(61) Bernhard, P.; Sargeson, A. M. *J. Chem. Soc., Chem. Commun.* **1985**, 1516−1518.
(62) Keene, F. R. *Coord. Chem. Rev.* **1999**, *187*, 121−149.
(63) Kuroda, Y.; Tanaka, N.; Goto, M.; Sakai, T. *Inorg. Chem.* **1989**, *28*, 2163−2169.
(64) Machkour, A.; Mandon, D.; Lachkar, M.; Welter, R. *Eur. J. Inorg. Chem.* **2005**, *1*, 158−161.
(65) Schwarz, F.; Schollhorn, H.; Thewalt, U.; Lippert, B. *J. Chem. Soc., Chem. Commun.* **1990**, 1282−1284.
(66) Douglas, A. E. *J. Phys. Chem.* **1955**, *59*, 109−110.
(67) Grimley, R. T.; Burns, R. P.; Inghram, M. G. *J. Chem. Phys.* **1961**, *34*, 664−667.

Scheme 2. Photofragmentation of Coordinated dmen[a]

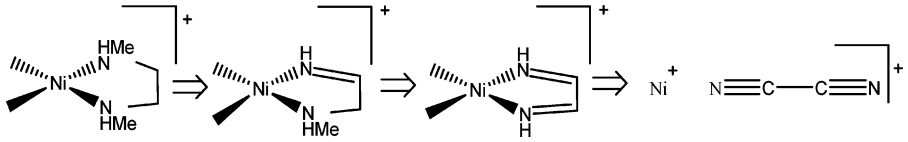

[a] Prominent peaks corresponding to mono- and diimine fragments attached to nickel are observed. Uncoordinated dicyanogen is formed in abundance.

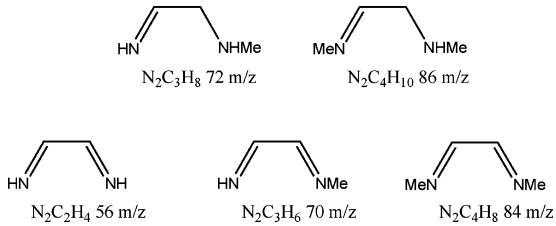

Figure 4. Structures of mono- and diimine fragments that could be formed by photofragmentation of methyl and hydrogen from dmen.

Table 1. Relative Ion Intensities of Significant Mass Peaks Observed during Photoexcitation of $Ni(tfa)_2(dmen)_2$ at 355 nm ($\sim 10^9$ W/cm^2), Listed per Column by Largest to Smallest Mass[a]

tfa lost		dmen lost		light fragments	
$Ni(tfa)-(N_2C_2H_4)_2$	64	$Ni(tfa)_2-(dmen)$	5	NiF	270
$Ni(tfa)-(dmen)$	18	$Ni(tfa)_2-(N_2C_3H_7)$	15	$N_2C_3H_7$	952
$Ni(dmen)_2$	33	$Ni(tfa)_2$	64	$N_2C_3H_6$	238
$Ni(N_2C_4H_8)_2$	19			CF_3	200
$Ni(N_2C_4H_8)$	15			Ni	sat
Ni(dmen)	36			NCCN	2786
$Ni(N_2C_3H_6)$	42			$N_2C_2H_4$	1905
$Ni(N_2C_3H_8)_2$	18			CF_2	429
Ni(dmen)−Me	24			CF	8345
				CH_3	6174
				C	8898

[a] Light fragments (<80 *m*/*z*) are always more dominant.

The second route begins with the loss of one tfa group and retention of both dmen ligands. The heaviest fragment in this pathway is $Ni(tfa)(dmen)_2^+$ at 347 *m*/*z*. Subsequent steps involve fragmentation within the dmen ligands; mass peaks of the formula $Ni(tfa)(N_2C_{2-4}H_{0-12})(N_2C_{2-4}H_{0-10})^+$ are observed throughout the high mass region from 275 to 347 *m*/*z*. If the tfa is photolabilized, then mass peaks of the formula $Ni(N_2C_{2-4}H_{4-12})_{1,2}^+$ are observed from 128 to 234 *m*/*z*. It is notable that when two dmen-based ligands remain coordinated but fragment internally, the resulting fragments are identical. The majority of peaks in the mass spectra belong to this second pathway and may be a result of the stability of the bidentate dmen ligand (chelate effect). Loss of a bidentate ligand requires two NiN bonds to be cleaved, whereas the loss of a monodendate tfa requires the cleavage of just a single NiO bond. It is remarkable that in both the tfa loss and dmen loss pathways, the nickel−nitrogen bonds and the main dmen ring remain intact while the substituent hydrogens and methyls photodissociate.

2. Formation of Stable Mono- and Diimine Fragments from dmen. A common feature of both the tfa loss and dmen loss pathways is that dmen always forms the same types of smaller fragments, mono- and diimine species. Figure 4 shows the structures of the five different types of imines (two mono- and three diimines) that are observed, and Table 1 lists the ions formed in each pathway and their relative intensities. Photofragmentation with 355 nm irradiation produces new metal complexes containing imines and diimines coordinated to nickel. Further fragmentation can lead to very stable organic cations (56, 70, and 72 *m*/*z*). They dissociate via methyl and hydrogen loss until dicyanogen (52 *m*/*z*) is eventually produced in significant yield (Scheme 2). Alternatively, dmen can lose one nitrogen atom and form organic products with mass peaks below 50 *m*/*z*. To be certain that all of these fragments originate from dmen, TOF mass spectra were taken of uncoordinated dmen at 355 nm (not shown). All of the mono- and diimine fragments that are illustrated in Figure 4 are also observed from fragmentation of the free ligand. A plausible explanation for the observed formation of mono- and diimines in the gas phase is the formation of double bonds leading to enhanced bond strength about the NCCN ring.

Scheme 3. Proposed Intramolecular Rearrangements That Bring Fluorine into Proximity of Nickel Leading to Diatomic NiF Formation

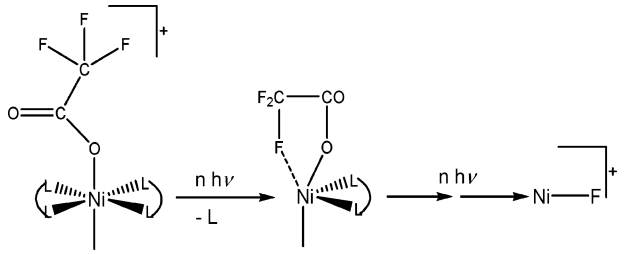

3. Mechanism for NiF^+ Formation. NiF^+ is observed under all excitation wavelengths even though there are no Ni−F bonds in the starting material. Fluorine abstraction has been reported to occur easily in the gas-phase photodissociation of transition metal hexafluoroacetylacetonate complexes (Cr(III), Ni(II), Cu(II), and Pt(II)).[49] The mechanism that was proposed involved metal−ligand bond cleavage, rotation about a C−C bond that brings the CF_3 molecule into proximity with the metal, and M−F formation with F−C bond breakage. In the case of trifluoroacetate, the mechanism for fluorine abstraction may be similar but simpler (Scheme 3). Following dmen loss, rotation about the C−O single bond can bring the CF_3 group close enough to the metal center that fluorine abstraction can occur. Indeed, there is a thermodynamic driving force for the formation of NiF; the reported bond energy is 101.4 kcal/mol.[68]

Summary

The photodissociation of gaseous $Ni(tfa)_2(dmen)_2$ consists of surprisingly rich intramolecular photochemical processes. Unlike solution-phase photochemistry of coordination compounds where the most common reaction is ligand loss, in the gas phase there are multiple pathways. The parent molecule either retains both dmen groups while losing one

(68) Gaydon, A. G. *Dissociation Energies and Spectra of Diatomic Molecules*, 3rd ed.; Chapman & Hall: London, 1968.

tfa ligand or retains both tfa molecules while one dmen completely dissociates. Both routes share something very unexpected: dmen forms stable mono- and diimine species both while attached to nickel and as free cations. This unique photochemistry is uncommon and rare in the gas phase. Also unexpected is the intramolecular rearrangement of the Ni−tfa entity resulting in the formation of diatomic NiF^+ which is always observed. The mechanism of fluorine abstraction may be similar to that reported for transition metal β-diketonates. Although fluorine incorporation into metal thin films is undesirable, $Ni(tfa)_2(dmen)_2$ may still prove to be a viable photo-assisted CVD precursor for nickel thin films considering the dominant ion yield of Ni^+ at all excitation wavelengths studied. To explore this further, experiments are currently underway.

Acknowledgment. This work was made possible by a grant from the National Science Foundation (CHE-0507929).

Supporting Information Available: Master list of all ions formed with relative intensities, TOF mass spectra under visible excitation at various wavelengths, and power law plots from which photon dependences were derived. This material is available free of charge via the Internet at http://pubs.acs.org.

IC061969C